PRAMANA
— journal of
physics

Vol. 64, No. 6
June 2005
pp. 991–1000

Colloidal interactions in two-dimensional nematic emulsions

N M SILVESTRE[1,2], P PATRÍCIO[2,3] and M M TELO DA GAMA[1,2]
[1]Departamento de Física da Faculdade de Ciências; [2]Centro de Física Teórica e Computacional, Universidade de Lisboa, Avenida Professor Gama Pinto 2, P-1649-003 Lisboa Codex, Portugal
[3]Instituto Superior de Engenharia de Lisboa, Rua Conselheiro Emídio Navarro 1, P-1949-014 Lisboa, Portugal
E-mail: margarid@cii.fc.ul.pt

Abstract. We review theoretical and experimental work on colloidal interactions in two-dimensional (2D) nematic emulsions. We pay particular attention to the effects of (i) the nematic elastic constants, (ii) the size of the colloids, and (iii) the boundary conditions at the particles and the container. We consider the interactions between colloids and fluid (deformable) interfaces and the shape of fluid colloids in smectic-C films.

Keywords. Colloids; nematics; topological defects.

PACS Nos 82.70.Dd; 77.84.Nh; 61.30.Jf

1. Introduction

In the last ten years, there has been continued interest in colloidal dispersions in nematics and other liquid crystalline phases (LCs) owing to their novel, complex behavior [1]. The behavior of spherical isotropic particles in a nematic matrix depends upon (i) the elastic constants of the nematic, (ii) the size of the particle, and (iii) the boundary conditions at the particle and the container, including the anchoring energy of the nematogenic molecules and possibly other (generic) surface tension effects. All of these contributions are temperature dependent and their combination leads to complex anisotropic long-ranged colloidal interactions [2–4]. These were reported to lead to a variety of novel self-organized colloidal structures, such as linear chains [5,6], periodic lattices [7], anisotropic clusters [3], and cellular structures [8] that are stabilized, in general, by topological defects.

More recently, two-dimensional (2D) inverted nematic emulsions were also studied and similar behavior has been found [9–13]. In particular, Landau–de Gennes (LdG) theory predicts that the stable configuration for a colloidal disk, with strong homeotropic anchoring, is always a pair of 1/2 charge topological defects [14] and thus the long-range interaction between 2D colloids is quadrupolar for any colloidal size [13].

In this paper we review recent results for the interactions between nematic colloids in 2D geometries. In particular, we discuss the interaction of circular colloids with deformable nematic–isotropic (NI) interfaces and preliminary results for the shape of fluid (deformable) colloids in smectic-C films.

2. Models and numerics

The simplest theory of uniaxial nematic liquid crystals (see e.g., [15] and references therein) is the celebrated Frank–Oseen elastic theory [16, 17]. The free energy is written as a quadratic function of the director derivatives, $1/2 \int K_{ijkl} \nabla_i n_j \nabla_k n_l$, where K_{ijkl} is the stiffness tensor. In the bulk, only three of these terms are independent: corresponding to splay ($\nabla \cdot \mathbf{n}$), twist ($\mathbf{n} \cdot (\nabla \times \mathbf{n})$), and bend ($\mathbf{n} \times (\nabla \times \mathbf{n})$), distortions. A simplifying assumption that will be used here considers a single elastic constant, K.

Topological defects are associated with broken continuous symmetries. They occur due to competing ordering effects and are widely observed in condensed matter (e.g., see [18]). The degree of orientational order $S = \langle P_2(\cos\theta) \rangle$ [19] measures the fraction of oriented molecules in the nematic. In the vicinity of defects, S decreases from its bulk value S_b and vanishes exponentially within the defect core. In addition, biaxiality may occur close to defects. In this region the director exhibits strong variations and the continuum theory breaks down due to the divergence of the derivatives of $\mathbf{n}$ inside the defect cores [1].

These divergencies are avoided and the degree of orientational order and biaxiality are accounted for in the context of the LdG approximation. For a nematic a suitable order parameter is a traceless symmetric second rank tensor that may be written as

$$Q_{\alpha\beta}(\mathbf{r}) = S(\mathbf{r})(n_\alpha n_\beta - \delta_{\alpha\beta}/3) + \mathcal{B}(\mathbf{r})(l_\alpha l_\beta - m_\alpha m_\beta). \tag{1}$$

$S(\mathbf{r})$ and $\mathcal{B}(\mathbf{r})$ are the degree of orientational order and biaxiality, respectively, and the unit vectors $\mathbf{n}$, $\mathbf{l}$ and $\mathbf{m}$ form a local orthonormal triad. When the biaxiality is zero, $\mathbf{n}$ corresponds to the director field. The LdG free energy density is written in powers of the tensor order parameter and its derivatives and is the sum of bulk and elastic terms [15]:

$$f_\mathrm{bulk} = -\frac{A(T)}{2}\mathrm{Tr}\{\mathbf{Q}^2\} + \frac{B}{3}\mathrm{Tr}\{\mathbf{Q}^3\} + \frac{C}{4}\mathrm{Tr}\{\mathbf{Q}^2\}^2, \tag{2}$$

$$f_\mathrm{elastic} = \frac{L_1}{2}\partial_\gamma Q_{\alpha\beta}\partial_\gamma Q_{\beta\alpha} + \frac{L_2}{2}\partial_\beta Q_{\alpha\beta}\partial_\gamma Q_{\gamma\alpha}, \tag{3}$$

where $A(T)$ is a linear function of the temperature, and B and C are constants [20]; L_1 and L_2 are related to the Frank–Oseen elastic constants with $L_1 = K/(2S_\mathrm{b}^2)$ and $L_2 = 0$ in the one-constant approximation. The cubic term is responsible for the first order nature of the bulk transition and favors uniaxial nematics.

Specific treatments of the container walls control the anchoring of the liquid crystal molecules [21]. This characterizes the energy cost associated with deviations

of the director from a given preferred orientation ν at the surface. Defining a surface tensor order parameter $(Q_{\alpha\beta})_0 = S_0(\nu_\alpha\nu_\beta - \delta_{\alpha\beta}/3)$, this contribution to the surface energy may be written as

$$F_{\text{surface}} = \int \frac{W}{2}\text{Tr}\{(\mathbf{Q}-\mathbf{Q}_0)^2\}\text{d}S. \tag{4}$$

W is the anchoring strength. For simplicity, we will assume that S_0 is equal to the bulk order parameter. In most cases, anchoring at the walls is assumed strong enough to consider the nematic orientation fixed at those boundaries.

In the following we consider dispersions of colloidal particles in nematic and smectic-C liquid crystals. The director field follows from minimization of the total free energy with the constraint that $\mathbf{n}$ is a unit vector, or that $Q_{\alpha\beta}$ is traceless using a numerical scheme based on finite elements and adaptive meshes. Standard procedures are used to minimize the free energy with respect to, e.g. the tilt angle $\theta(\mathbf{r})$ or the tensor order parameter $Q_{\alpha\beta}$. Typical calculations start with meshes with hundreds of points and end with tens of thousands, yielding free energies with an accuracy of 10^{-4}. For details of the numerical calculations, see [22].

3. Colloidal interactions in 2D nematics

3.1 *Quadrupolar colloid–colloid interaction*

We consider the interaction between two parallel, infinitely long, colloidal particles of sectional radii a. We assume that the director is perpendicular (homeotropic anchoring) to the surface of the colloids and that the far-field director ($\mathbf{n}_\infty = \mathbf{n}(\infty)$) is parallel to the y-axis. For simplicity we neglect biaxiality and use the simpler tensor order parameter $Q_{\alpha\beta}(\mathbf{r}) = S(\mathbf{r})(n_\alpha n_\beta - \delta_{\alpha\beta}/2)$.

In 2D nematics, circular colloidal particles with strong homeotropic anchoring are surrounded by two 1/2 topological defects, symmetrically located near the surface of the colloid along the x-axis. If the separation between two such particles is large, the nematic distortion is approximately given by adding the isolated solutions and the long-range interaction energy exhibits quadrupolar symmetry [13]:

$$F_{\text{int}} \approx 6\pi K\left(r_{\text{d}}^4 + a^4\right)\frac{1-2\sin^2 2\alpha}{R^4}. \tag{5}$$

R is the separation between particles, α is their relative orientation with respect to the x-axis and r_{d} is the equilibrium distance of the defects from the center of the colloid. At small separations, the nematic deformation is no longer the sum of isolated quadrupolar solutions.

The effective interaction between disks is plotted in figure 1a as a function of the distance R between disks, at different orientations ($\alpha = 0,\ \pi/4,\ \pi/2$). The quadrupolar interaction is confirmed at large separations. However, at smaller separations, the free energy changes dramatically. Orientations that are repulsive at large separations (e.g., $\alpha = 0,\ \pi/2$) become attractive at different threshold distances ($R_{\text{th}} \approx 5a$ and $R_{\text{th}} \approx 3a$, respectively). This change in behavior is

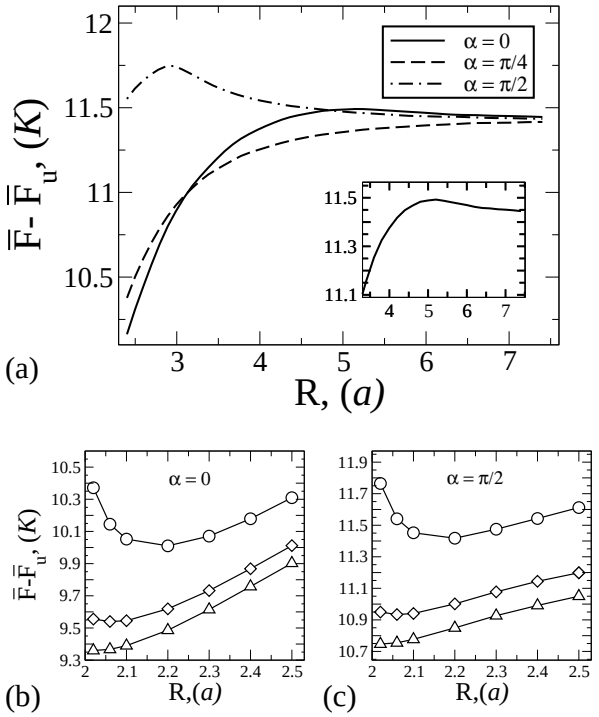

Figure 1. (**a**) Reduced elastic free energy $\bar{F} = F/K$ as a function of the distance R between disks, at different orientations ($\alpha = 0$, $\pi/4$, $\pi/2$). (Bottom) Reduced elastic free energy $\bar{F} = F/K$ as a function of the disks separation R, for three reduced anchoring strengths, $\omega = aW/K = 250, 10, 7.5$, corresponding to the circles, diamonds and triangles respectively. (**b**) Parallel alignment ($\alpha = 0$); (**c**) perpendicular alignment ($\alpha = \pi/2$). $F_u = F[S = S_b]$ is the Landau–de Gennes free energy of a uniform equilibrium nematic.

accompanied by the displacement of the defects [13]. At short distances, the free energy corresponding to the parallel orientation ($\alpha = 0$) becomes lower than the free energy of the long-range preferred oblique orientation ($\alpha = \pi/4$). At large R the disks prefer an oblique orientation (with $\alpha = \pi/4$), that changes to parallel (with $\alpha = 0$) as their separation decreases.

For strong homeotropic anchoring, and for all orientations α, we observed a repulsion when the disks are nearly at contact, at a separation $R \approx 2.1a$. We relaxed the strong anchoring condition and calculated the total elastic free energy as a function of the distance R between disks, for three reduced anchoring strengths ($\omega = aW/K = 250, 10, 7.5$). The results are plotted in figure 1. These anchorings are strong enough to nucleate defects in the nematic. The repulsion obtained at small separations for strong anchoring ($\omega = 250$) vanishes at a critical anchoring strength that lies between 7.5 and 10, i.e., $7.5 < \omega < 10$. We predict that below this critical anchoring coalescence of droplets will occur.

3.2 *Interactions with a NI interface*

Recent results [23] revealed that the drag on colloids by a moving NI interface plays an important role on the formation of different spatial patterns. Here, we consider a geometry similar to that used in the experiment. A uniform temperature gradient was imposed along the x-axis with the 'hot' wall at $x = L/2$ and the 'cold' wall at $x = -L/2$, where L is the size of the system. The director at the 'cold' wall is fixed either parallel or perpendicular to the wall. The order parameter at the 'hot' wall is set to zero. Note that the position of the interface, at $x = 0$, is pinned by the temperature gradient. A colloidal particle, which we take to be a long cylinder of radius R, with the symmetry axis parallel to the z-axis, is immersed in the nematic. We assume strong homeotropic anchoring of the director at the colloidal surface and that the nematic is uniaxial and it completely wets the colloid.

We studied the interaction of a colloid with the NI interface under various anchoring conditions: (i) director parallel at the NI interface, $L_2 > 0$; (ii) director perpendicular at the NI interface, $L_2 < 0$; (iii) director tilted with respect to the interface, due to a mismatch between interfacial anchoring and the alignment at the cell boundaries.

The results are qualitatively the same [24]. Here we describe the case where the anisotropy of the elastic constants is $L_2/L_1 = 2$, favoring director alignment parallel to the NI interface. The 'cold' wall along the y-axis, was also fixed parallel to the NI interface.

Typical order parameter and director maps are shown in figure 2. The strong anchoring of the director at the colloidal surface results in two half-integer defect lines in the nematic, far from the interface (see figure 2a). On reducing the colloidal distance from the interface, the defect closest to the interface merges (discontinuously) with the isotropic phase (figures 2b, 2c). The interface bulges towards the colloid to accommodate the isotropic phase, where the defect core disappeared. As the colloid moves further into the isotropic phase, it is wrapped by the NI interface that forms a nematic 'cavity' around the colloid (figure 2d). The second defect is still present on the nematic side. At a certain point, this configuration becomes metastable, and eventually annihilation of the second defect occurs. This is accompanied by a symmetry breaking transition: the cavity is no longer symmetric under $x \to -x$ reflexion (figure 2e illustrates one of the two possible configurations). These configurations with broken symmetry are always metastable. Finally, deep in the isotropic phase, the colloid is wrapped by a thin layer of nematic phase due to the (wetting) boundary conditions at the colloidal surface (figure 2f).

To investigate the nature of the structural transitions between different director field configurations, we plotted the free energy as a function of the particle position in figure 3. The jumps in the free energy reveal discontinuous (or first-order) instabilities between the physical director configurations. The equilibrium position, i.e., the position where the force on the colloid vanishes, is near the interface, at $x = 0$. Close to the minimum the free energy is a quadratic function of the position of the colloidal particle and thus, in this region, the force is linear or proportional to the colloid-interface separation d, i.e., $F = F_0 + k\frac{d}{R}$. Our numerical calculations reveal that, to a good approximation, $k \propto R^2$, in contrast with the scaling relation suggested before [23], based on an oversimplified model in which the NI interface was assumed to be flat.

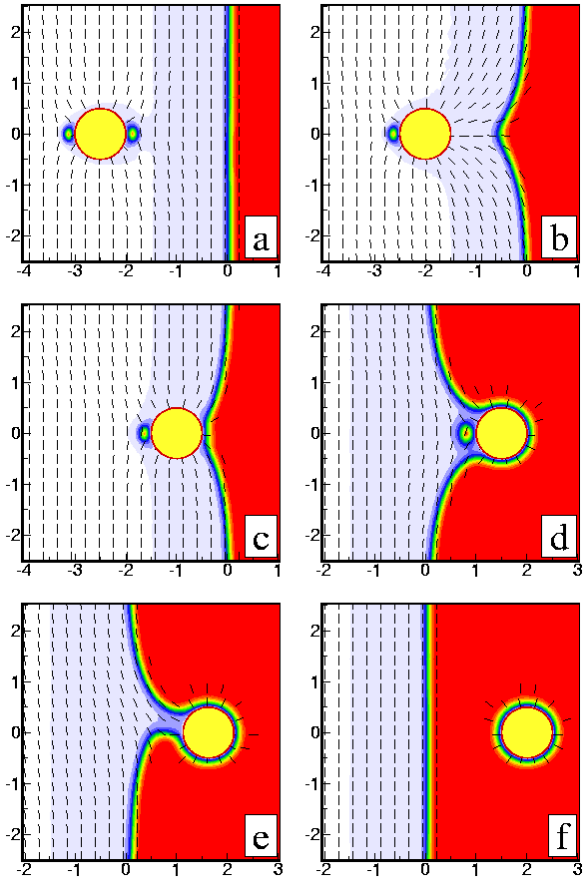

Figure 2. Order parameter and director maps for colloids at a distance, d, from the NI interface: (**a**) $d = -2.5$; (**b**) $d = -2$; (**c**) $d = -1$; (**d**) $d = 1.5$; (**e**) $d = 1.625$; (**f**) $d = 2$. Red corresponds to the isotropic phase, and white to the nematic phase. System size $L = 12$, anisotropy of the elastic constants $L_2/L_1 = 2$. Lengths are in units of the size of the colloidal particle, $2R = 1$.

4. Colloidal interactions in smectic-C films

In thin films of smectic-C liquid crystals molecular ordering is closely related to nematic-like monolayer films. Although the nematic symmetry, $n \rightarrow -n$, is no longer present, the projections of the tilted molecules play the role of nematogens [18]. The behavior of inclusions in smectic-C films was studied recently both theoretically [9] and experimentally [10, 11]. In what follows we review results for the dipolar interactions between colloidal particles dispersed in free-standing films of smectic-C*, where the molecules are chiral. We also present preliminary results for the shape of nematic colloids in smectic-C films.

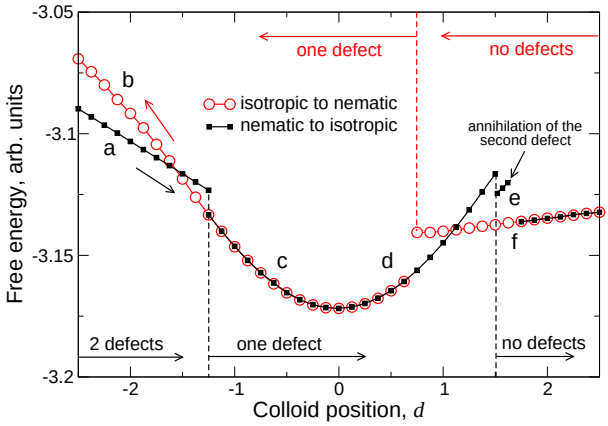

Figure 3. Free energy F as a function of the distance of a colloidal particle from the NI interface. Both metastable and stable solutions are shown. (■): particle moving from the isotropic to the nematic phase; (○): particle moving from the nematic to the isotropic phase. The letters a–f indicate the configurations described earlier, represented in figure 2.

4.1 *Dipolar colloid–colloid interaction*

We start with two circular colloids, with homeotropic anchoring, in 2D smectic-C* films. We expect each colloid to nucleate a single topological defect and pairs of colloids and defects to interact through long-range dipolar interactions [9]. The colloids will then form chains, with the particles separated by topological defects [10].

We have used the Frank–Oseen free elastic energy (one elastic constant approximation) and considered two circular disks of radius a separated by a distance R along the x-axis. The far-field director was taken parallel to the x-axis and homeotropic boundary conditions were imposed at the colloidal surfaces. On the x-axis, the far-field director was oriented horizontally everywhere.

We found that the energy was minimized by the pinning of one of the defects between the colloidal disks and that the separation of the disks had no influence on the position of the outer defect. The latter was pinned at a distance $r_{\mathrm{d_o}} = 1.41a$ from the nearest particle. When considering the equilibrium position of the inner defect $r_{\mathrm{d_i}}$, as a function of the disk separation R, we observed three different regimes [12]. At small disk separation ($R \leq 2.82a$) the defect is at the mid-point between the disks, $r_{\mathrm{d_i}} = R/2$. In an intermediate regime ($2.82a \leq R \leq 6.5a$) the defect position varies non-monotonically with R. Finally, at large disk separations the position of the inner defect is independent of R and is given by that of an isolated disk.

The Frank–Oseen free energy exhibits a pronounced minimum at $R = (2.82 \pm 0.01)a$ (see figure 4a), comparable to the experimental value of $(2.6 \pm 0.2)a$ [10]. The signature of the dipolar interaction at large disk separations is seen in figure 4b.

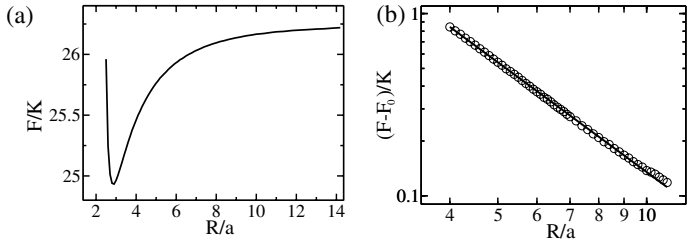

Figure 4. (**a**) The 2D Frank–Oseen free energy as a function of the disk separation. The free energy has a pronounced minimum at $R = (2.82 \pm 0.01)a$; (**b**) log–log plot of the interaction free energy vs. disk separation. F_0 is the free energy at infinite separation. Circles represent the numerical results. The line is proportional to R^{-2}.

4.2 *Nematic inclusions in smectic-C films*

Recently, Cluzeau and co-workers [11] studied the interaction between inclusions of nematic in smectic-C films. Observations show that the molecules of the smectic-C film align parallel to the surface of the colloids (planar anchoring). Also, two topological defects nucleated at the surface of each particle on opposite sides aligned along the far-field direction. These are called boojums. The presence of boojums induces colloidal interactions with quadrupolar symmetry and several structures (linear and branched chains and two-dimensional patterns) have been observed depending on the concentration of colloids. It was also found that, depending on size, the shape of the colloids may differ significantly from circular. Small colloids are elliptical while larger ones are almost circular. In this section, we discuss preliminary results for the shape of colloidal particles with planar anchoring conditions dispersed in smectic-C films.

In smectic-C films the nematic symmetry is no longer present. This means that the tensor order parameter previously introduced is not appropriate. The smectic-C order parameter includes both the tilt angle θ and the azimuthal orientation Φ, as $\phi = \theta \exp\{i\Phi\}$ [25]. Due to the polar symmetry of the order parameter the bulk third-order term is no longer present. After various simplifications, the reduced LdG free energy may be written as

$$\tilde{F} = \int \left[|\phi|^2 \left(|\phi|^2 - 1 \right) + \xi^2 |\nabla \phi|^2 \right] \mathrm{d}S + \int \left[\gamma + \Delta \left(|\phi_0|^4 - \mathrm{Re}\{\phi_0^* \phi\}^2 \right) \right] \mathrm{d}l. \quad (6)$$

Here ξ is the correlation length. The line integral is over the boundary of the colloid and takes into account the interfacial tension contribution. γ and Δ are, respectively, the isotropic and anisotropic interfacial tensions and ϕ_0 is the order parameter at the boundary of the particle. Note that when $\phi = \phi_0$ the surface term reduces to the Rapini–Papoular form. The behavior of an isolated colloid is controlled by the parameters $\tilde{\omega} = R_0 \Delta / \xi^2$ and $\tilde{\sigma} = \gamma / \Delta$.

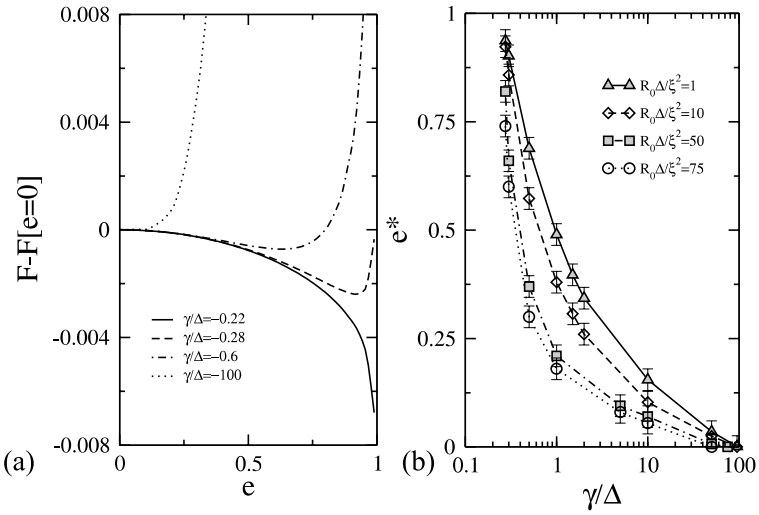

Figure 5. (**a**) Reduced Landau–de Gennes free energy as a function of eccentricity, for $\tilde{\omega} = 1$. $F[e = 0]$ is the free energy for circular colloids. (**b**) Preferred eccentricity, e^*, as a function of $\tilde{\sigma}$.

In order to determine under what conditions the shape of the colloid differs from a circle, we consider the colloid to be elliptical with eccentricity e. In figure 5a we plot the LdG free energy as a function of the eccentricity of the colloid, for $\tilde{\omega} = 1$ and several values of $\tilde{\sigma}$ ($\tilde{\sigma} = -0.22,\ -0.28,\ -0.6,\ -100$). For each choice of the parameters, the minimum of the energy defines the preferred eccentricity e^*. In figure 5b we have also plotted the preferred eccentricity as a function of $\tilde{\sigma}$, for several values of $\tilde{\omega}$. The preferred eccentricity drops rapidly with increasing $\tilde{\sigma}$ and this drop becomes stronger as $\tilde{\omega}$ increases. The results suggest that below $\tilde{\sigma} \sim 0.25$ the preferred eccentricity is one, although numerical problems prevented us from checking this limit.

5. Conclusions

We have shown that finite elements with adaptive meshes are very useful to study problems involving widely different length scales, such as colloidal nematic emulsions where inhomogeneities occur on microscopic (defects) and mesoscopic (colloids) length scales. The numerical techniques can be extended to three (or more) colloidal particles and to arbitrary three-dimensional geometries, although the numerics become considerably more demanding.

References

[1] H Stark, *Phys. Rep.* **351**, 387 (2001)
[2] S Ramaswamy, R Nityananda, V Raghunathan and J Prost, *Mol. Cryst. Liq. Cryst.* **288**, 175 (1996)

[3] P Poulin and D A Weitz, *Phys. Rev.* **E57**, 626 (1998)
[4] T C Lubensky, D Pettey, N Currier and H Stark, *Phys. Rev.* **E57**, 610 (1997)
[5] P Poulin, H Stark, T C Lubensky and D A Weitz, *Science* **275**, 1770 (1997)
[6] J-C Loudet, P Barois and P Poulin, *Nature (London)* **407**, 611 (2000)
[7] V G Nazarenko, A B Nych and B I Lev, *Phys. Rev.* **87**, 075504 (2001)
[8] S P Meeker, W C K Poon, J Crain and E M Terentjev, *Phys. Rev.* **E61**, R6083 (2000)
[9] D Pettey, T C Lubensky and D R Link, *Liq. Cryst.* **25**, 5 (1998)
[10] P Cluzeau, P Poulin, G Joly and H T Nguyen, *Phys. Rev.* **E63**, 031702 (2001)
[11] P Cluzeau, G Joly, H T Nguyen and V K Dolganov, *JETP Lett.* **75**, 482 (2002)
[12] P Patricio, M Tasinkevych and M M Telo da Gama, *Euro. Phys. J.* **E7**, 117 (2002)
[13] M Tasinkevych, N M Silvestre, P Patrício and M M Telo da Gama, *Euro. Phys. J.* **E9**, 341 (2002)
[14] J Fukuda and H Yokoyama, *Euro. Phys. J.* **E4**, 389 (2001)
[15] P G de Gennes and J Prost, *The physics of liquid crystals*, 2nd ed. (Clarendon Press, Oxford, 1993)
[16] F C Frank, *Disc. Faraday Soc.* **25**, 19 (1958)
[17] C Oseen, *Trans. Faraday Soc.* **29**, 883 (1933)
[18] D R Nelson, *Defects and geometry in condensed matter physics* (Cambridge University Press, Cambridge, 2002)
[19] P M Chaikin and T C Lubensky, *Principles of condensed matter physics* (Cambridge University Press, Cambridge, 1995)
[20] L D Landau and E M Lifshitz, *Statistical physics*, 2nd ed. (Pergamon, Oxford, 1969)
[21] A A Sonin, *The surface physics of liquid crystals* (Gordon and Breach Publishers, Luxembourg, 1995)
[22] N M Silvestre, P Patrício, M Tasinkevych, D Andrienko and M M Telo da Gama, *J. Phys. Condens. Matter* **16**, S1921 (2004)
[23] J L West, A Glushchenko, G Liao, Y Reznikov, D Andrienko and M P Allen, *Phys. Rev.* **E66**, 012702 (2002)
[24] D Andrienko, M Tasinkevych, P Patrício and M M Telo da Gama, *Phys. Rev.* **E69**, 021706 (2004)
[25] D H Van Winkle and N A Clark, *Phys. Rev.* **A38**, 1573 (1988)